Early Detection of Osteoarthritis Using Local Binary Patterns: A Study Directed at Human Joint Imagery

Kwankamon Dittakan[1] and Frans Coenen[2]

[1] Faculty of Technology and Environment,
Prince of Songkla University, Phuket Campus,
80 Moo 1, Vichit-Songkram Road, Kathu, Phuket, Thailand
[2] Department of Computer Science,
University of Liverpool, Liverpool, L69 3BX, United Kingdom
{kwankamon.d@phuket.psu.ac.th,coenen@liverpool.ac.uk}

Abstract. Osteoarthritis (OA) is a chronic health condition that causes severe joint pain and stiffness; it is a major cause of disability in older people. The risk of OA increases from age 45 and older. Early diagnosis is typically made using X-ray imagery. In this paper an automated mechanism for OA screening is proposed. The fundamental idea is to generate a classifier that is able to distinguish between OA or non-OA images. The challenge is how bast to translate an X-ray image into a form that serves to both captures key information while remaining compatible with the classification process. It is suggested that image texture is the most desirable feature to be considered. The process is filly described and evaluated. The data used for the evaluation was obtained from the right Tibia of 50 female subjects. Excellent results were obtained, recorded AUC values of 1.0.

Keywords: Data Mining, Image Classification, Medical Image Analysis and Mining, Osteoarthritis Screening

1 Introduction

Osteoarthritis (OA) is a degenerative joint disease causing joint inflammation and consequently joint pain and stiffness. OA is a major cause of disability amongst older people (over the age of 45). In (Arthritic Research UK, 2013) it was reported that 8.75 millions people in the UK have sought treatment for OA (5 millions in women and 3.5 million in men). World wide figures are not available as not all countries specifically record instance of OA. However, in (Tanna, 2004), it was estimated that (worldwide) 9.6% of men and 18% of women aged over 60 have "symptomatic OA". Given the ageing global population, the prevalence of OA is anticipated to increase. The OA condition is typically diagnosed by a doctor or clinician by clinical examination supported by X-ray or Magnetic resonance imaging (MRI). Early diagnosis, before external symptoms present themselves, can be conducted using X-ray and MRI imagery. The physical signs of OA include: joint tenderness, creaking or grating (crepitus) sounds, bony swelling, excess fluid, reduced movement, joint instability and muscle thinning (Zahurul et al., 2010).

In this paper a mechanism for automating the process is proposed founded on the concept of medical image analysis. More specifically a process for the early detection

of OA is proposed founded on the use of the idea classification applied to human bone imagery. To act as a focus for the work X-ray images of the right Tibia were considered. The fundamental idea is to generate a classifier, using labelled X-ray image data, which can then be applied to detect OA. The dataset used to evaluate the proposed framework was composed of a set of X-ray images obtained from the right Tibia of 50 women, of which 25 were from control (non-OA) individuals and the remaining 25 were from clinically diagnosed OA patients. The main objective of the work presented in this paper is thus to classify X-ray image as being either OA or non-OA with respect to the nature of the presented X-ray image data. The proposed approach offers a number of advantages: (i) speed of processing, (ii) automation (unlikely to to be subject to human error) and (iii) low cost.

The main challenge for X-ray image classification (and medical image mining in general) is identifying the most appropriate representation for the input X-ray images; the representation needs to capture key information while remaining compatible with the classification process. Note that without modern Multi-core Computing the medical image of interests are typically too large to be used in their entirety. The idea presented in this paper is thus to use the a texture representation to capture the image data. More specifically the Local Binary Pattern (LBP) concept (Pietikäinen, 2005). The proposed process is filly described and evaluated.

The reminder of the paper is organised as follows. In Section 2 some related work is briefly presented. An overview of the proposed framework for the early detection of OA is presented in Section 3. Section 4 describes the adopted image texture-based representation. The nature of the classification mechanism used is presented in Section 5. Section 6 reports on the evaluation of the proposed framework. Finally, a summary, some conclusions and suggestions for future work are discussed in Section 7.

2 Related Work

Digital imagery has been increasingly use for medical diagnosis; consequently medical digital images have become of increasing significance to health care. There are a number of image capture mechanisms that can are commonly used, including: (i) X-ray, (ii) Computerised Tomography (CT), (iii) Magnetic Resonance Imaging (MRI), (iv) Ultrasound, (v) Positron Emission Testing (PET) and (vi) Single Photon Emission Computed Tomography (SPECT) (Alattas and Barkana, 2015). Example medical application domains, where medical image data has been utilised, include: (i) the identification conditions such a epilepsy using MRI brain data (Udomchaiporn et al., 2014) and detection and (ii) the classification of brain tumours according to whether they are malignant or benign (Nasir et al., 2014).

Computer-based screening for OA, using medical image data, has not been widely available. In (Soh et al., 2014) a mechanism was reported, with respect to knee OA (the most common form of OA), whereby images were segmented using shape analysis algorithms. A similar approach was used in (Ababneh and Gurcan, 2010) but in this case a graph-cut strategy was adopted. In both cases MRI images were used, work has also been reported where X-Ray image data was used (Shamir et al., 2009), as in the case of this paper.

It is worth noting that image analysis is also an important and fundamental component with respect to other analysis domains such as computer vision and pattern recognition where the main goal is to understand the characteristics of an image and interpret its semantic meaning. Image classification is an emerging image analysis technique whereby image classifiers (predictors) are built using pre-labelled training data. The performance of such classifiers depends on: (i) the quality of the training data and (ii) the nature of the preprocessing applied to capture the embedded image information. With respect to the latter the idea is to identify features within the training set in order to define a feature vector space representation. Image features of interest can be categorised into two groups: (i) general features and (ii) domain-specific features (Han and Ma, 2002). General features are application independent features such as: (i) colour, (ii) texture and (iii) shape. Domain-specific features are application dependent features, such as elements of the human face when considering face recognition.

With respect to the work presented in this paper a representation used in the context of texture analysis was used. Texture is an important feature with respect to both human and computer vision. There are three principle mechanisms that may be adopted to describe texture in digital images: (i) statistical, (ii) structural and (iii) spectral. The statistical mechanism is concerned with the capture of texture using quantitative measures such as "smoothness", "coarseness" and "graininess". Using structural mechanisms image texture is described using a set of texture primitives or elements (texels) that occur as regularly spaced or repeating patterns. In the case of the spectral mechanism the image texture features are extracted by using the properties of the Fourier spectrum domain so that "high-energy narrow peaks" in the spectrum can be identified (Gonzalez and Woods, 2007). The usage of Local Binary Patterns (LBPs), the mechanism adopted with respect to the work presented in this paper, is a texture representation strategy which is both statistical and structural in nature (Pietikäinen, 2005). Using the LBP approach a binary number is produced, for each pixel, by thresholding its value with its neighbouring pixels. LBPs offer advantages of robustness with respect to illumination changes and computational simplicity. The LBP method has been used with respect to many image analysis application domains such as face recognition (Hadid, 2008), (Zhao and Pietikainen, 2007). Because of their significance in the context of the work presented in this paper, LBPs are discussed in further detail in Section 4.

3 Proposed Framework

The proposed framework for the generation of the desired OA classifier is presented in this section. A schematic of the framework is given in Figure 1. The framework comprised three phases (as represented by the rectangular boxes): (i) image representation, (ii) feature discretisation and selection and (iii) classifier generation. The input to the first phase is a collection of X-ray images that have been pre-labeled using domain experts. Recall that each X-ray image has to be represented in an appropriate manner that ensures that the salient features are maintained while at the same time supporting classifier generation. The left rectangular box in Figure 1 is where the image translation is conducted; the input data is translated into a LBP-based representation, which can then

be combined to define a feature space from which feature vectors can be generated. Once the feature vectors have been generated feature discretisation and selection are applied (the centre rectangular box in Figure 1) in order to reduce the overall size of the feature space by reducing the number of attribute-values to be considered and by pruning those features that do not serve to discriminate significantly between classes. Feature discretisation and selection is considered in further detail in Section 5 below. With respect to the work presented in this paper, the Chi-squared feature selection method was used. Classifier model generation is the third phase in the proposed framework (the right rectangular box in Figure 1) during which the desired classifier is generated (also discussed further in Section 5 below).

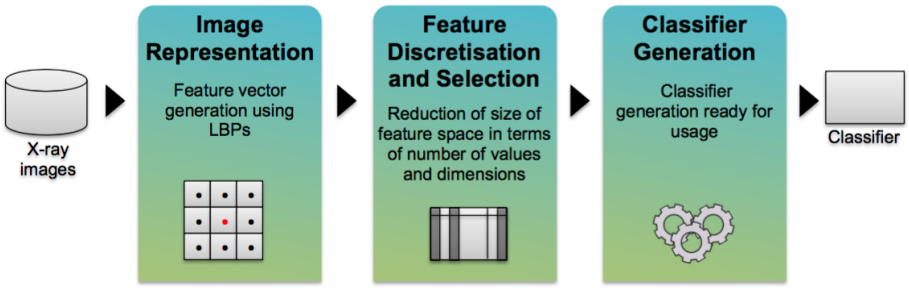

Fig. 1: Schematic illustration the proposed OA classifier generation framework

4 Local Binary Pattern Based Representation.

Local Binary Patterns (LBPs) have been widely applied in the context of image processing and computer vision applications where it is important to capture texture information. Examples include: (i) texture segmentation and classification (Chen and Chen, 2002), (ii) object detection (Heikkila and Pietikainen, 2006) (in images) and (iii) image segmentation (Kachouie and Fieguth, 2007), (Wu et al., 2014). The LBP concept, in the context of image texture analysis, was first introduced by (Ojala et al., 2002). The major advantages pf LBPs are there simplicity, ease of generation and robustness to rotation and monotonic transformation of the adopted colour scale. The fundamental idea is to define each pixel in an image according to its eight cardinal and sub-cardinal neighbours. To generate a set of LBPs from an X-ray image the image is first converted into a linear colour representation, the greyscale representation in our case, if not already in this form. A 3×3 pixel window is then used and moved over the image, with the current pixel at the centre, the centre pixel's greyscale value is then compared with its eight neighbouring greyscale values. If the neighbouring greyscale value is greater than the centre pixel greyscale value a 1 is recorded, otherwise a 0 is recorded (Heusch et al., 2006). In this manner an eight digit binary number is defined describing each pixel according to its 3×3 pixel neighbourhood. In other words 256 (2^8) different patterns can be described. The process is demonstrated in Figure 2.

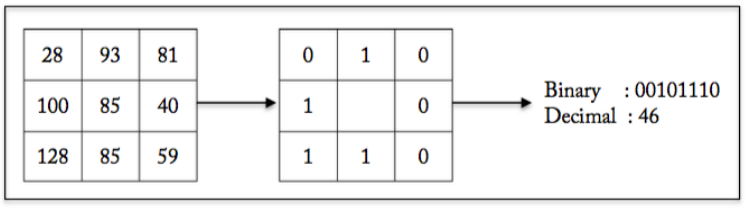

Fig. 2: LBP generation

More formally we can describe an LBP in terms of an ordered set of binary comparisons of greyscale values between the centre pixel of the window with its eight surrounding neighbourhoods. The process can be expressed as shown in Equation 1:

$$LPB(x_c, y_c) = \sum_{n=0}^{7} f(i_n - i_c)2^n \tag{1}$$

where i_c is the greyscale value of the centre pixel (x_c, y_c), i_n is the greyscale value of a neighbourhood pixel and $f(x)$ is defined according to Equation 2 below:

$$f(x) = \begin{cases} 1, if\ x \geq 0 \\ 0, if\ x < 0 \end{cases} \tag{2}$$

In the example given in Figure 2, a 3×3 immediate neighbourhood is considered. However, variations of the basic LBP concept can be produced by: (i) using different *radii of neighbourhoods* (R) and/or (ii) different numbers of sampling points (P). The variations can be described using the notation $LBP_{P,R}$. With respect to the work presented in this paper $P = 8$ and a range of values for R was used. Some examples variations are shown in Figure 3. With reference to the figure: (i) $LBP_{8,1}$ equates to 8 sampling points within a radius of 1 (Figure 3(a)), (ii) $LBP_{8,2}$, equates to 8 sampling points within a radius of 2 (Figure 3(b)), and (iii) $LBP_{8,3}$, equates to 8 sampling points within a radius of 3 (Figure 3(c)). Note that we kept the value of P constant at 8 because this conveniently resulted in a 8 bit integer. Alternatives might have been $P = 4$ or $P = 16$.

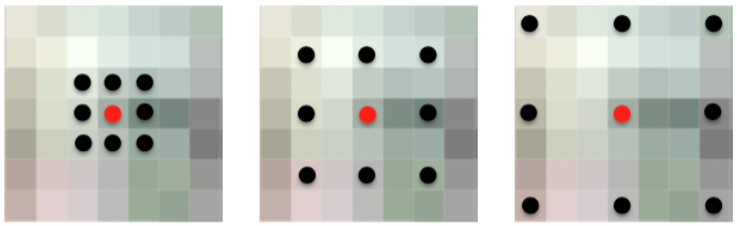

Fig. 3: LBP variations

A set of LBPs can be visualised as a histogram with 256 "bins" on the X-axis, and occurrence count on the Y-axis. Alternatively we can think of a set of LBPs as defining

a 256 dimensional feature space, where each element represents a potential LBP value which has an occurrence count associated with it. The latter is the conceptualisation used in this paper.

5 Feature Discretisation, Selection and Classification

Once a collection of LBPs have been identified (as described above) the next step in the framework (Figure 1) is feature discretisation and selection. However, before this could be commenced data discretisation was applied so as to reduce the number of values in each dimension in the feature space; in other words the continuously valued attributes were converted into a set of ranged attributes. The number of ranges was set to 10 as this was felt to provide a sufficient level of distinction while still considerably reducing the overall number of values to be considered. Feature selection was then applied so as to reduce the number of dimensions in the feature space, but in such a way that the reduced set still provided for a good discrimination between classes. The Chi-squared feature selection mechanism was used with respect to the work presented later in this paper. Note that, in common with many other feature selection techniques, Chi-squared feature selection requires a parameter k, the maximum number of "best" features to be selected.

When the feature selection was completed the images were represented in terms of a set of feature vectors drawn from the reduced feature space to which any number of different classifier generators could be applied. With respect to the evaluation presented later in this paper five classifier generation machine learning methods were considered: (i) Naive Bayes, (ii) Decision Tree (C4.5), (iii) Sequential Minimal Optimisation (SMO), (iv) Back Propagation Neural Networks and (v) Logistic Regression. The implementations used were those available in the Waikato Environment for Knowledge Analysis (WEKA) machine learning workbench (Witten et al., 2011).

6 Evaluation

The evaluation of the proposed approach to OA screening is presented in this section. Extensive evaluation was conducted with respect to the proposed approach. This section reports on only the most significant results obtained (there is insufficient space to allow for the presentation of all the results obtained). The evaluation was conducted by considering a specific case study directed at digital X-ray images taken from the right Tibia of 50 women. In each case the entire X-ray image was not used for the analysis, as it was known that clinicians consider only two particular areas within these X-rays. These two different areas were identified and extracted from the X-rays in the form of sub-images which could be used in isolation or combination. Further detail concerning this image pre-processing is provided in Sub-section 6.1. The overall aim of the evaluation was to provide evidence that the OA condition can be easily detected using the proposed approach. To this end four sets of experiments were conducted with the following objectives:

1. To determine whether if it was better to use the derived sub-images in isolation or in combination.

2. To determined the most appropriate LBP representation with respect to the three variations described in Sub-section 6.3.
3. To identify the most appropriate value for the Chi-squared feature selection k parameter, the maximum number of features to be retained.
4. To provide a comparison of the effectiveness of a number of classifier generation methods. To this end a selection of different classifier generators, taken from the Waikato Environment for Knowledge Analysis (WEKA) machine learning workbench (Witten et al., 2011), was used.

Each of the above objectives is discussed in further detail in Sub-sections 6.2 to 6.5 below in the context of the results obtained. Ten fold Cross-Validation (TCV) was applied throughout and performances recorded in terms of: (i) accuracy, (ii) area under the ROC curve (AUC), (iii) sensitivity, (iv) specificity and (v) precision. The results presented in the tables included in the following four sub-sections are thus all averages over ten runs of cross validation.

6.1 Tibia X-ray Image Data Sets

For the evaluation, as already noted, a training set comprising 50 X-ray images was used represented in greyscale using the DICOM (Digital Image and Communication on medicine) format for X-ray images, a commonly used format in Computed Radiography (CR). An example is given in Figure 4. The X-ray images were obtained from the right Tibia of 50 women. The data set comprised: (i) 25 control images and (ii) 25 OA images. For each image two sub-images were extracted referred to as the medial and lateral sub images (highlighted in Figure 4. Detail of these two sub images are given in Figures 5(a) and 5(b). From Figures 5(a) and 5(b) it is noticeable that it is not obvious that we can detect anything very much from these images. However, it was clear that the sub-images could be used in isolation or in combination. Therefore three individual data sets were created: (i) medial, (ii) lateral and (iii) medial and lateral. The later was generated simply by concatenating the feature vectors from the first two.

6.2 Sub-Image Usage (Individual v. Combination)

This sub-section considers the first of the evaluation objectives, whether it is better to consider the derived sub-images in isolation or in combination. For the experiments the $LBP_{8,3}$ representation was used together with $k = 50$ for the "Chi-squared" feature selection and Logistic regression classification (because experiments reported on later in this paper had indicated that these produced good results). The results are presented in Table 1 (highest values indicated in bold font). From the table it can be observed that best result was obtained by using the sub-images in combination, a best recorded AUC value of 1.000 and sensitivity value of 1.000. Although the sub-images used in isolation also produced reasonable results. Thus, in conclusion, pairing the sub-images makes sense (the more data the better). It should also be noted here that clinicians who analyse Tibia X-ray images typically consider both areas (medial and lateral), thus the results confirm this practice.

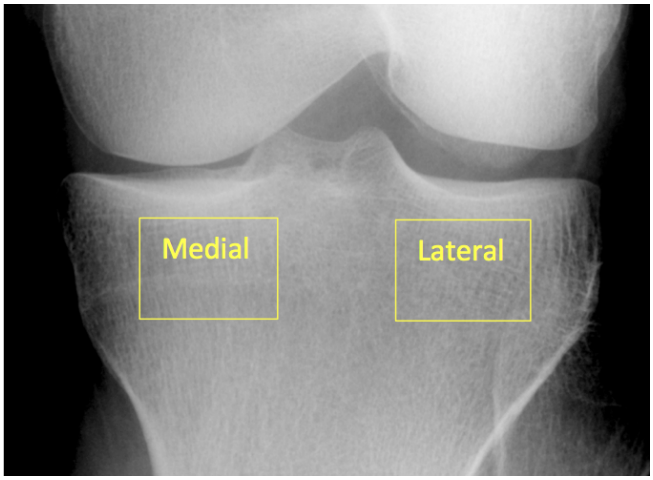

Fig. 4: Examples of right Tibia X-ray image.

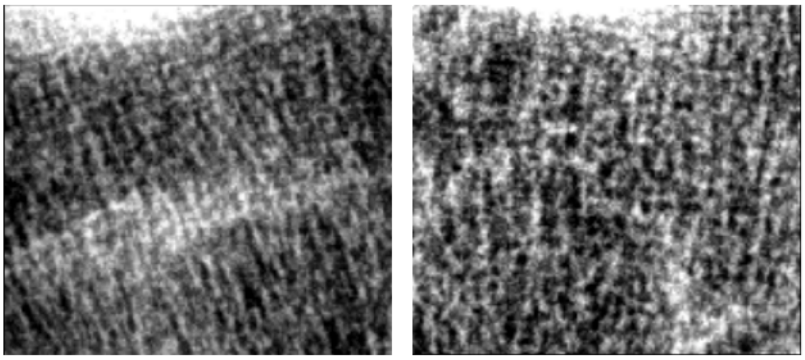

(a) An example of Medial image (b) An example of Lateral image

Fig. 5: Example sub-images, (a) medial and (b) lateral (b).

Table 1: Results using sub-images in isolation and in combination.

Image set	Accuracy	AUC	Sensitivity	Specificity	Precision
Medial dataset	0.960	0.984	0.960	0.960	0.960
Lateral dataset	0.940	0.994	0.940	0.940	0.941
Medial and Lateral	**1.000**	**1.000**	**1.000**	**1.000**	**1.000**

6.3 LBP Representation

In Sub-section 4 it was noted that variations of the LBP representation can be defined in terms of the values P and R, where P is the number of sampling points and R is the neighbourhood radius; the notation $LBP_{P,R}$ was used to indicate particular variations. This section reports on the evaluation conducted to compare the operation of a range of LBP variations with increasing values of R (P was kept constant because this conveniently resulted in an eight bit integer). For the experiments the combined sub-image dataset was used because previous experiments, reported above in Sub-section 6.2, had indicated that this produced the best performance. Again $k = 50$ was used for the Chi-squared feature selection, together with Logistic regression classification. The results are presented in Table 2 (best results shown in bold font). From the table it can be seen that best results started to be encountered using $\text{LBP}_{8,3}$ ($R = 3$); a recorded AUC value of 1.000 and a sensitivity value of 1.000. This continued until $LBP_{8,8}$ was reached when effectiveness started to diminish. There is no clear reason for the anomalous results when using $LPBP_{8,6}$ other than some undefined vagary of the data set. The results indicating that lower values of R did not serve to encapsulate the most effective level of detail. Similarly when R gets too large detail is again lost. It was thus concluded that $LBP_{8,3}$ was the most appropriate LBP variation to adopt.

Table 2: Results Using Alternative LBP representations

Representation	Accuracy	AUC	Sensitivity	Specificity	Precision
$\text{LBP}_{8,1}$	0.980	0.989	0.980	0.980	0.981
$\text{LBP}_{8,2}$	0.980	**1.000**	0.980	0.980	0.981
$\text{LBP}_{8,3}$	**1.000**	**1.000**	**1.000**	**1.000**	**1.000**
$\text{LBP}_{8,4}$	**1.000**	**1.000**	**1.000**	**1.000**	**1.000**
$\text{LBP}_{8,5}$	**1.000**	**1.000**	**1.000**	**1.000**	**1.000**
$\text{LBP}_{8,6}$	0.980	**1.000**	0.980	0.980	0.981
$\text{LBP}_{8,7}$	**1.000**	**1.000**	**1.000**	**1.000**	**1.000**
$\text{LBP}_{8,8}$	0.980	0.988	0.980	0.980	0.981

6.4 Best Value for k

This section reports on the evaluation conducted to identify a best value for K with respect to the adopted Chi-squared feature selection method. For the evaluation a sequence of experiments was conducted using a range of k values from 30 to 70 incrementing in steps of 10. For the evaluation the combined sub-image dataset was again adopted together with the the $\text{LBP}_{8,3}$ variation (because experiments reported in Sub-sections 6.2 and 6.3 had shown that these produced the best results). Logistic regression classification was also again used. The obtained results are presented in Table 3 (best results highlighted in bold font). From the table it can be observed that $k = 50$ produced the best outcomes with respect to all the evaluation metrics considered (a best recorded AUC value of 1.000 and sensitivity of 1.000). Note that accuracy, sensitivity, specificity and precision "drop off" either side of $k = 50$.

Table 3: Results using a range of different values for k with respect to Chi-squared feature selection

k	Accuracy	AUC	Sensitivity	Specificity	Precision
$k = 30$	0.960	0.997	0.960	0.960	0.963
$k = 40$	0.960	0.980	0.960	0.960	0.960
$k = 50$	**1.000**	**1.000**	**1.000**	**1.000**	**1.000**
$k = 60$	0.980	**1.000**	0.980	0.980	0.981
$k = 70$	0.980	**1.000**	0.980	0.980	0.981

6.5 Classification Learning Methods

There are many different kinds of classification paradigms to select from, with no obvious best paradigm for texture-based image classification. This sub-section presents a comparative analysis of a number of these in the context texture-based Tibia X-ray image analysis: (i) Naive Bayes, (ii) Decision Tree, (iii) Sequential Minimal Optimisation (SMO), (iv) Back Propagation Neural Networks and (v) Logistic Regression. For the analysis the combined sub-image dataset was used together with the the $LBP_{8,3}$ variation and $k = 50$ (because earlier reported experiments had shown that these produced the best results). The results of the comparative analysis are presented in Table 4. From the Table it can be observed that, with the exception of decision tree classification, the remaining four selected classifiers all produced good performances. However, best results were obtained using Logistic Regression (AUC value of 1.000 and sensitivity value of 1.000).

Table 4: Results using a range of Classification Learning methods

Classifier generation methods	Accuracy	AUC	Sensitivity	Specificity	Precision
Naive Bayes	0.980	**1.000**	0.980	0.980	0.981
Decision Tree (C4.5)	0.680	0.725	0.680	0.680	0.685
SMO	0.980	0.980	0.980	0.980	0.981
Neural Networks	0.960	0.998	0.960	0.960	0.960
Logistic Regression	**1.000**	**1.000**	**1.000**	**1.000**	**1.000**

7 Conclusions

A framework for the early detection of Osteoarthritis (OA) from X-ray imagery has been presented. The significance is that this can be used for national screening programmes. The main idea presented in this paper is to construct a classification model based on the texture features of X-ray sub-images, which can then be used to predict the OA condition. The key element with respect to this process is the way in which individual X-ray sub-images are represented so that an effective classifier can be generated. To this end the Local Binary Pattern (LBP) texture representation mechanism was adopted with which to encode the sub-image content. To evaluate the proposed approach experiments were conducted using a collection of 50 test datasets obtained from the right Tibia of 50 women (these had been hand-labelled by trained clinicians). The main findings evidenced by the reported evaluation were:

– The proposed approach was extremely effective, AUC and sensitivity scores of 1.000 were regularly recorded.
– Practitioners, in the context of Tibia X-ray images, concentrate on two areas within such images (referred to as the medial and lateral areas). Sub-images were extracted with respect to both these areas and experiments conducted using these sub-images in isolation and in combination; as anticipated using these sub-images in combination produced the best results (a recorded average AUC value of 1.000).
– The most appropriate LBP variation, out of the the variations considered, was $LBP_{8.3}$ (recorded AUC value of 1.000).
– The most appropriate k value to be used with respect to Chi-squared feature selection was found to be $k = 50$, in other words the best fifty LBP dimensions should be selected.
– In the context of the most appropriate classification methods to be adopted experiments were conducted using five different classification paradigms. The best performing was to be Logistic regression (again evidenced by AUC results of 1.000).

Thus, in conclusion, the proposed approach produced excellent results indicating a good "way forward" with respect to OA screening. A criticism that might be directed at the presented work is that the evaluation data set was relatively small comprising 50 X-ray images from which 100 sub-images were extracted (the evaluation data set featured a $50:50$ class distribution). For the future work the research team thus intends to conduct further experiments using larger datasets.

References

Ababneh, S. and Gurcan, M. (2010). An efficient graph-cut segmentation for knee bone osteoarthritis medical images. In *Electro/Information Technology (EIT), 2010 IEEE International Conference on*, pages 1–4.

Alattas, R. and Barkana, B. (2015). A comparative study of brain volume changes in alzheimer's disease using mri scans. In *Systems, Applications and Technology Conference (LISAT), 2015 IEEE Long Island*, pages 1–6.

Arthritic Research UK (2013). Osteoarthritis in general practice — data and perspectives. Technical report, Arthritic Research UK, Copeman House, St Marys Gate, Chesterfield, S41 7TD.

Chen, K.-M. and Chen, S.-Y. (2002). Color texture segmentation using feature distributions. *Pattern Recogn. Lett.*, 23(7):755–771.

Gonzalez, R. C. and Woods, R. E. (2007). *Digital Image Processing*. Pearson Prentice Hall, Third edition.

Hadid, A. (2008). The Local Binary Pattern approach and its applications to face analysis. In *Proceedings of the First Workshop on Image Processing Theory, Tools and Applications (IPTA)*, pages 1–9. IEEE Computer Society.

Han, J. and Ma, K. (2002). Fuzzy color histogram and its use in color image retrieval. *IEEE Transactions on Image Processing*, 11(8):944–952.

Heikkila, M. and Pietikainen, M. (2006). A texture-based method for modeling the background and detecting moving objects. *IEEE Trans. Pattern Anal. Mach. Intell.*, 28(4):657–662.

Heusch, G., Rodriguez, Y., and Marcel, S. (2006). Local binary patterns as an image preprocessing for face authentication. In *Proceedings of the Seventh IEEE International Conference on Automatic Face and Gesture Recognition (FGR)*, pages 9–14. IEEE Computer Society.

Kachouie, N. and Fieguth, P. (2007). A medical texture local binary pattern for trus prostate segmentation. In *Engineering in Medicine and Biology Society, 2007. EMBS 2007. 29th Annual International Conference of the IEEE*, pages 5605–5608.

Nasir, M., Khanum, A., and Baig, A. (2014). Classification of brain tumor types in mri scans using normalized cross-correlation in polynomial domain. In *Frontiers of Information Technology (FIT), 2014 12th International Conference on*, pages 280–285.

Ojala, T., Pietikainen, M., and Maenpaa, T. (2002). Multiresolution gray-scale and rotation invariant texture classification with local binary patterns. *IEEE Transactions on Pattern Analysis and Machine Intelligence*, 24(7):971–987.

Pietikäinen, M. (2005). Image analysis with local binary patterns. In *Proceedings of the Conference on Scandinavian conference on Image Analysis (SCIA)*, pages 115–118, Heidelberg. Springer-Verlag Berlin.

Shamir, L., Ling, S., Scott, W., Bos, A., Orlov, N., Macura, T., Eckley, D., Ferrucci, L., and Goldberg, I. (2009). Knee x-ray image analysis method for automated detection of osteoarthritis. *Biomedical Engineering, IEEE Transactions on*, 56(2):407–415.

Soh, S., Swee, T. T., Ying, S. S., En, C. Z., bin Mazenan, M., and Meng, L. K. (2014). Magnetic resonance image segmentation for knee osteoarthritis using active shape models. In *Biomedical Engineering International Conference (BMEiCON), 2014 7th*, pages 1–5.

Tanna, A. (2004). Osteoarthritis "opportunities to address pharmaceutical gap". Technical report, World Health Organisation Archive.

Udomchaiporn, A., Coenen, F., García-Fiñana, M., and Vanessa Sluming, V. (2014). 3-d MRI brain scan classification using A point series based representation. In *Data Warehousing and Knowledge Discovery - 16th International Conference, DaWaK 2014, Munich, Germany, September 2-4, 2014. Proceedings*, pages 300–307.

Witten, I. H., Frank, E., and Hall, M. A. (2011). *Data Mining: Practical Machine Learning Tools and Techniques*. Morgan Kaufmann, Amsterdam, Third edition.

Wu, C., Lu, L., and Li, Y. (2014). A study on pattern encoding of local binary patterns for texture-based image segmentation. In *Machine Learning and Cybernetics (ICMLC), 2014 International Conference on*, volume 2, pages 592–596.

Zahurul, S., Zahidul, S., and Jidin, R. (2010). An adept edge detection algorithm for human knee osteoarthritis images. In *Signal Acquisition and Processing, 2010. ICSAP '10. International Conference on*, pages 375–379.

Zhao, G. and Pietikainen, M. (2007). Dynamic texture recognition using local binary patterns with an application to facial expressions. *Proceedings of the IEEE International Conference on Pattern Analysis and Machine Intelligence (TPAMI)*, 29(6):915–928.